

ORIGINAL RESEARCH PAPER

Synthesis of Highly Effective Novel Graphene Oxide-Polyethylene Glycol-Polyvinyl Alcohol Nanocomposite Hydrogel For Copper Removal

Eman Serag¹, Ahmed El-Nemr^{1,*}, Azza El-Maghraby²

¹Marine Pollution Department, Environmental Division, National Institute of Oceanography and Fisheries, Kayet Bey, El-Anfoushy, Alexandria, Egypt

² Fabrication Technology Department, Advanced Technology and New Materials Institute, City for Scientific Research and Technology Application, Alexandria, Egypt

Received: 2017-08-03

Accepted: 2017-09-14

Published: 2017-10-15

ABSTRACT

A novel Graphene oxide-polyethylene glycol and polyvinyl alcohol (GO-PEG-PVA) triple network hydrogel were prepared to remove Copper(II) ion from its aqueous solution. The structures, morphologies, and properties of graphene oxide (GO), the composite GO-PEG-PVA and PEG-PVA were characterized using FTIR, X-ray diffraction, Scanning Electronic Microscope and Thermal Gravimetric analysis. A series of systematic batch adsorption experiments were conducted to study the adsorption property of GO, GO-PEG-PVA hydrogel and PEG-PVA hydrogel under different conditions (e.g. pH, contact time and Cu^{2+} ions concentration). The high adsorption capacity, easy regeneration, and effective adsorption-desorption results proved that the prepared GO-PEG-PVA composite hydrogel could be an effective adsorbent in removing Cu^{2+} ion from its aqueous solution. The maximum adsorption capacities were found to be 917, 900 and 423 mg g^{-1} for GO-PEG-PVA hydrogel, GO and PEG-PVA hydrogel, respectively at pH 5, 25 °C and Cu^{2+} ions' concentration 500 mg l^{-1} . The removal efficiency of the recycled GO-PEG-PVA hydrogel were 83, 81, 80 and 79% for the first four times, which proved efficient reusability.

Keywords: Copper; Graphene Oxide; Hydrogel; Polyethylene Glycol; Polyvinyl Alcohol

How to cite this article

Serag E, El-Nemr A, El-Maghraby A. Synthesis of Highly Effective Novel Graphene Oxide-Polyethylene Glycol-Polyvinyl Alcohol Nanocomposite Hydrogel For Copper Removal. J. Water Environ. Nanotechnol., 2017; 2(4): 223-234. DOI: 10.22090/jwent.2017.04.001

INTRODUCTION

Heavy metals are considered of great concern due to their extreme toxicity even at low concentrations because of their tendency to accumulate in organisms and the food chain [1]. The disposal of wastewater indiscriminately is an environmental problem worldwide due to the negative impacts of polluted water on human health [2]. Effluents of industries such as chemical, metallurgical, mining, and dyeing, as well as battery manufacturing that contain different types of toxic heavy metal ions such

as As, Cd, Co, Cr, Ni, Hg, and Pb [1-4]. Therefore, it is necessary to treat industrial effluents contaminated by heavy metals prior to their discharge into the environment [5, 6]. Different sorbent materials have been prepared and studied extensively to remove heavy metal ions [7-11].

Although many techniques were employed for the treatment of wastewater containing heavy metals, it is important to report that the selection of the most suitable treatment method for metal removal from wastewater depends on different parameters such

* Corresponding Author Email: ahmed.m.elnemr@gmail.com

as pH, metal concentration, environmental impact and economics parameter [1-3].

Graphene oxide (GO) is of great interest as a result of its low price, easy access, and graphene conversion ability. Graphene can be prepared by oxidation of graphite to graphene oxide to intersperse the carbon layers with oxygen molecules and then reduce GO to separate the carbon layers completely into individual or a few layers to give graphene. Therefore, graphene oxide is a by-product of this process, because when the oxidizing agents react with graphite, the inter-planar spacing between the layers of graphite increases. The completely oxidized graphite can be dispersed in a base solution such as water to produce graphene oxide [12-14]. Also, different studies have been made for photodegradation and waste treatment [15-18].

The primary synthetic method of GO is the conventionally-modified Hummers method, where proportional amounts of oxidants, such as KMnO_4 , NaNO_3 and concentrated H_2SO_4 , are mixed in order with the graphite [19]. Considering the new functional groups that have been introduced to the surface of GO and its high surface area, the GO nano-sheets should have a high-sorption capacity of heavy metal ions from their aqueous solutions [19].

The GO chitosan composite powders [20], chitin GO hybrid composite [21] and GO chitin composite foams [22] have been prepared for metal ions and dye removals. However, it is somewhat tough to separate the GO powder adsorbents from wastewater due to their high solubility and dispersibility, which may lead to secondary environmental problems. Therefore, it is very urgent to synthesize and design stable composite materials that are easy to separate expediently and efficiently from the treated wastewater, as well as easy to regenerate without much complication.

Poly (vinyl alcohol) (PVA) is a water-soluble polymer with non-toxicity, biocompatibility and biodegradability characteristics. Hence, PVA has been manufactured into a variety of adsorbent types, such as ion-exchange film and hydrogel [23]. PVA is a semi-crystal hydrophilic polymer consisting of one hydroxyl group in each repeat unit and that representing desirable adsorbent structure. Like other hydrogels, the PVA hydrogel shows faster adsorption kinetics for removing heavy metals from aqueous solution [24]. PEG, as a biodegradable synthetic material, shows good

biocompatibility and low immunogenicity and it is nontoxic. PEG is soluble in both water and many organic solvents [25].

In this work, we aim to synthesize graphene oxide and a novel nano-composite graphene oxide-polyethylene glycol and polyvinyl alcohol (GO-PEG-PVA) hydrogel to use in the safe removal of water pollutants without leaving any toxic residual. GO and synthesized composite hydrogel were separately investigated as adsorbents for the removal of Cu(II) ions from water through batch adsorption.

MATERIAL AND METHOD

Chemicals and reagents

Graphite Flakes (acid treated 99%, Asbury Carbons), sodium nitrate (98%, Nice Chemicals), potassium permanganate (99%, RFCL), hydrogen peroxide (30% wt, Emplura), sulphuric acid (98%, ACS), PVA (molecular weight, 72,000; degree of hydrolysis, 98.0–98.8 mol %) and polyethylene glycol were purchased from Sigma-Aldrich Company. Copper sulphate pentahydrate and glutaraldehyde were obtained from a local company and used without further purifications.

Synthesis of graphene oxide (GO)

Modified Hummer's method was used in the synthesis of graphene oxide from graphite powder [13]. In brief, 1.0 g of graphite and 0.5 g of NaNO_3 were well mixed together and then 23 ml of concentrated H_2SO_4 was added slowly under constant stirring. After stirring for 1 hour, 3 g of KMnO_4 was added in portions to the solution while keeping the reaction temperature below 20 °C to prevent overheating and explosion. Then, the obtained reaction mixture was stirred at about 35 °C for 12 hours followed by adding 500 ml of distilled water in the presence of vigorous stirring. The reaction mixture was left to react at 98 °C for 40 minutes further. That was then followed by adding 50 ml of 30% H_2O_2 drop by drop. The reaction mixture was cooled, centrifuged and washed with 1N HCl aqueous solution to remove the metal ions and further washed with double distilled water until the solution pH reached 6.5. The resulting yellow-brown graphene oxide solid was dried under reduced pressure for 24 hours (Fig. 1) [26, 27].

Preparation of Hydrogel

GO-PEG-PVA hydrogel was synthesized by fully dissolving 10.0 g of PVA in 100 ml of double distilled

water at a temperature of 90 °C under magnetic stirring. Then, it was left to cool down to room temperature. That was later followed by adding 100 mg of GO under vigorous magnetic stirring. 5 ml of PEG was added to the reaction mixture, followed by a cross-linking using 10 ml of 2.5% glutaraldehyde solution in 1% HCl, which acted as the cross-linking agent and catalyst, respectively. Stirring continued for 15 minutes. The reaction mixture was kept in an oven at 80 °C to produce the GO-PEG-PVA hydrogel (Fig. 2a) [28]. PEG-PVA hydrogel without GO was also prepared following the same method for comparison (Fig. 2b).

Characterization techniques

The samples were characterized by FTIR spectra using Bruker VERTEX 70 spectrophotometer with ATR platinum unit, and X-ray diffraction analysis

using XRD-7000, Shimadzu Corp., Columbia, MD that operated with Cu Ka radiation (λ D 0.154060 nm) that was generated at 30 kV and 30 mA. Scans were done at 2° min^{-1} for 2θ values between 10 and 100 degrees. Thermogravimetric analysis was obtained using TGA50 Shimadzu, Japan. This measurement was carried out at a heating rate of $10^\circ \text{ C min}^{-1}$ and under nitrogen gas. The morphologies of the samples were observed under Scanning Electron Microscope (JEOL, Model JSM 6360LA, Japan).

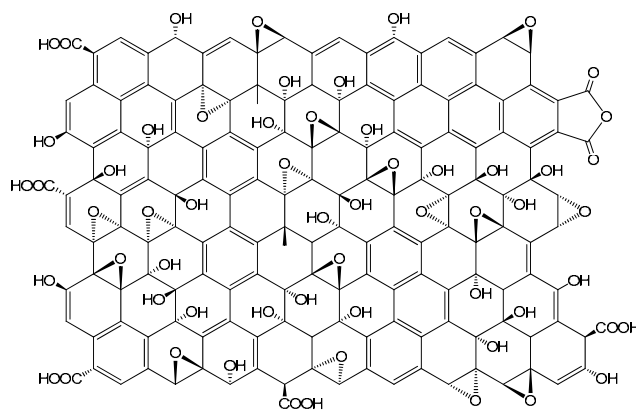
Adsorption Experiments

Preparation of stock solution

1.978 g of copper sulfate pentahydrate ($\text{CuSO}_4 \cdot 5\text{H}_2\text{O}$) was dissolved in 1,000 ml of double distilled water to prepare the stock solution of 500 mg l^{-1} . The other solutions with different



(a)



(b)

Fig. 1: (a) Photographic image of as-prepared GO solution (b) Proposed model of GO structure.



(a)



(b)

Fig. 2: (a) Photographic image of PVA-PEG-GO hydrogel (b) photographic image of PVA-PEG hydrogel

concentrations were obtained by successive dilution. The pH of the solutions was adjusted using 1.0M HCl or 1.0M NaOH.

Batch adsorption experiment

In typical batch experiments with GO (100 mg), the hydrogel corresponds to 100 mg GO while the hydrogel without GO (the control which had been carried out to correct any adsorption of metal on PVA or PEG surface) swelled in 100 ml of standard solution. A concentration of 500 mg l⁻¹ of Cu²⁺ ions on a rotary shaker at 150 rpm and 250 ml capped conical flasks were all employed under the required contact time at room temperature (25°C ± 1°C). The collected samples were filtered through 0.45 micron filters and the concentration of Cu²⁺ ions was immediately determined through a UV Spectrophotometer (Analyticjena Spekol 1300 UV-VIS Spectrophotometer, Model No 45600-02, Cole Parmer Instrument Co., USA) using 1-(2-pyridylazo)-2-naphthal (PAN) solution at the maximum wavelength λ_{\max} for the colored complex solution; the result was determined at 550 nm [29].

The effect of pH was studied at different pH values (1, 3, 5 and 7) at initial Cu²⁺ ion concentration of 500 mg l⁻¹ and 100 mg dosage of GO, the hydrogel corresponded to 100 mg GO and to that without GO. The effect of contact time on Cu²⁺ ions removal was conducted by studying the removal percentage at different times from 10 to 100 minutes using the dosage of 100 mg GO and hydrogel with and without GO at the optimum pH 5.

To investigate the effect of Cu²⁺ ions' initial concentration, the experimental work was conducted at Cu²⁺ ion initial concentration between 50 to 500 mg l⁻¹ dosages at pH 5 for 60 minutes. A number of Cu²⁺ ions adsorbed at equilibrium q_e (mg g⁻¹) were calculated using the following equation 1 [28].

$$q_e = \frac{(C_0 - C_e) \times V}{m} \quad (1)$$

Where C_0 , represents the initial ion concentration (mg g⁻¹), C_e is the equilibrium Cu²⁺ ion concentration (mg g⁻¹), m is the mass (g) of the adsorbent and V is the solution volume in L.

For the recyclability experiment, the adsorbed Cu²⁺ ions on the adsorbent were eluted with 0.1 M HCl solution. The adsorbent was then treated with 0.1 M NaOH solution to neutralize the hydronium ion (H₃O⁺) on the GO-PVA-PEG gel, and the adsorbent was further washed with deionized

water. The regenerated GO-PVA-PEG gel was reused in the next cycle of the sorption experiment. All the experimental work was performed in duplicates and the relative standard deviation was less than 5%.

RESULT AND DISCUSSION

Synthesizing graphene oxide from graphite was achieved by the modified Hummer's method which demonstrated a less hazardous and more efficient way for graphite oxidation [30, 31]. Graphene oxide individual sheets can be viewed as they are decorated with different types of oxygen functional groups on both sides of the plane and around the edges [32, 33]. The ionization of carboxyl groups presented at the edges of graphene oxide sheet can electrostatically stabilize the graphene oxide in water, alcohols and certain organic solvents to form a colloidal suspension without surfactants (Fig. 1) [34-36].

The newly formed double network hydrogel may be considered a good adsorbent mainly due to the following advantages: (1) GO greatly improves the strength of the hydrogel, which makes it easy to regenerate and (2) the existence of oxygen-containing groups in the hydrogel network provides plenty of active sites able to adsorb different types of heavy metal ions.

The satisfactory heavy metals adsorption performance, good reusability, and relatively low cost reveal the potential of PVA-PEG-GO gel for practical application. GO-PEG-PVA is a novel network nanocomposite and these polymers have very good ability to swell and adsorb of heavy metals as well as they are biodegradable and nontoxic.

Characterization

The FTIR spectrum of GO (Fig. 3a) shows a broad peak between 3353 cm⁻¹ in the high-frequency area together with a sharp peak at 1629 cm⁻¹, this corresponds to the stretching and bending vibrations of OH groups, and of water molecules adsorbed on the graphene oxide. Therefore, it can be concluded that GO has strong hydrophilicity [37]. Absorption peak observed at 1715 cm⁻¹ represents C=O carbonyl group, while the stretching at 1130 and 1038 cm⁻¹ represents the C-O epoxide group [38]. Finally, the peak observed at 877 cm⁻¹ can be attributed to the stretching vibration of C=C. The presence of these peaks corresponding to the presence of oxygen-containing function groups, prove the oxidation of the graphite to graphene

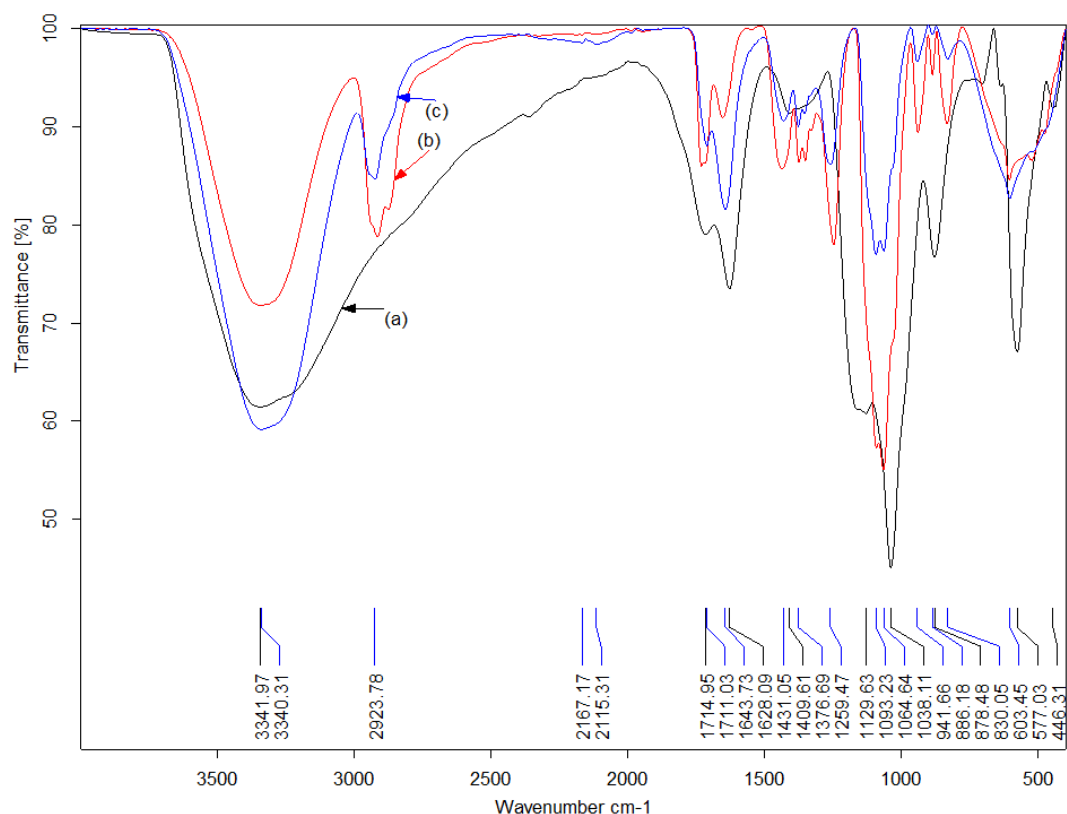


Fig. 3: FTIR Spectrum of (a) Graphene Oxide, (b) GO-PEG-PVA hydrogel and (C) PVA-PEG hydrogel.

oxide. The presence of polar groups, such as surface hydroxyl, led to the formation of hydrogen bonds between GO and water molecules; this further explains the hydrophilic nature of graphene oxide [39]. FTIR analysis is one of the most powerful techniques to investigate polymeric systems because it provides information on both polymer-polymer interactions and blends compositions using those vibrational modes attributed to the free and hydrogen bonded carbonyl and hydroxyl groups [40]. Theoretically, hydrogen bonding and/or other secondary interactions occurring between the functional groups on dissimilar polymers should cause a shift in the peak position of these participating functional groups. This behavior is shown by blending miscible polymers that exhibit extensive phase mixing. Stretching frequencies of the participating functional groups usually shifted with the hydrogen bonding interactions towards a lower wave-number; they showed an increase in peak intensity and broadening. The shift in peak position also depends on the strength of the interaction [40]

Fig. 3b,c show FTIR of synthesized hydrogels. The stretching band of hydroxyl groups in PVA in the composite hydrogels is observed at 3340 cm^{-1} as a broadband which indicates the presence of a high degree of intramolecular and intermolecular hydrogen bonding in the hydrogel network [40, 41]. The peak at 2914 cm^{-1} in Figs. 4b,c is the characteristic band of alkyl (CH_2) groups of both PVA and PEG. The stretching vibrational band of $\text{C}=\text{O}$ group at 1730 cm^{-1} is attributed to the aldehyde group, while $\text{C}=\text{C}$ groups appeared at 1650 cm^{-1} . The absorption band at 1436 cm^{-1} is assigned as CH_2 bending vibration while the deformation vibration of $\text{C}-\text{CH}_3$ is associated with the absorption band at 1351 cm^{-1} [40]. The peak at 1247 cm^{-1} is due to the $\text{C}-\text{O}$ stretching mode, which is a contribution from both the PVA and PEG. The stretching at 1065 cm^{-1} represent the epoxide groups; it was also observed that the intensity of the peak in the case of a hydrogel containing GO, is higher than that of the hydrogel without GO. The vibrational band at 1093 cm^{-1} is mostly attributed to the crystallinity of the PVA, where it is related to carboxyl stretching band ($\text{C}-\text{O}$) [42].

Fig. 4 shows the X-ray diffraction pattern (XRD) of GO that had been synthesized by the modified Hummer's method. The sharp diffraction peak observed at $2\theta = 11.02^\circ$ corresponds to the (001) diffraction peak of GO. The distance of GO's interlayer was calculated using Bragg's Law (Eq. 2).

$$d_{\text{spacing}} = \frac{\lambda}{2\sin\theta} \quad (2)$$

θ is Bragg's angle in radians and λ is X-ray's wavelength (0.1542 nm) [43]. The calculated interlayer spacing of GO was 0.71 nm, which is a large interlayer distance and might be an indication to the formation of functional groups, such as hydroxyl, epoxy and carboxyl groups [44]. The XRD curves of the PVA-PEG and PVA-PEG-GO nano-composites

are presented in Fig. 4b. One of the major factors that affect the polymer mechanical properties is the crystallinity. The XRD pattern of the pure PVA membranes revealed strong crystalline reflections at around $2\theta = 19.92^\circ$ and a shoulder at 22.74° . That represented reflections at 101 and 200 at the monoclinic unit cell, results that are characteristic of PVA [45]. In the XRD profile of PVA-PEG-GO nano-composite hydrogel, the intensity of PVA diffraction peaks decreased (Fig. 4b).

The SEM micrographs of synthesized GO with different scale bars are given in Fig. 5a, which shows that the graphene oxide has a layered structure that can afford ultrathin and homogeneous graphene films. Such films are continuous or folded at times and it is possible to see the individual sheet edges, including the

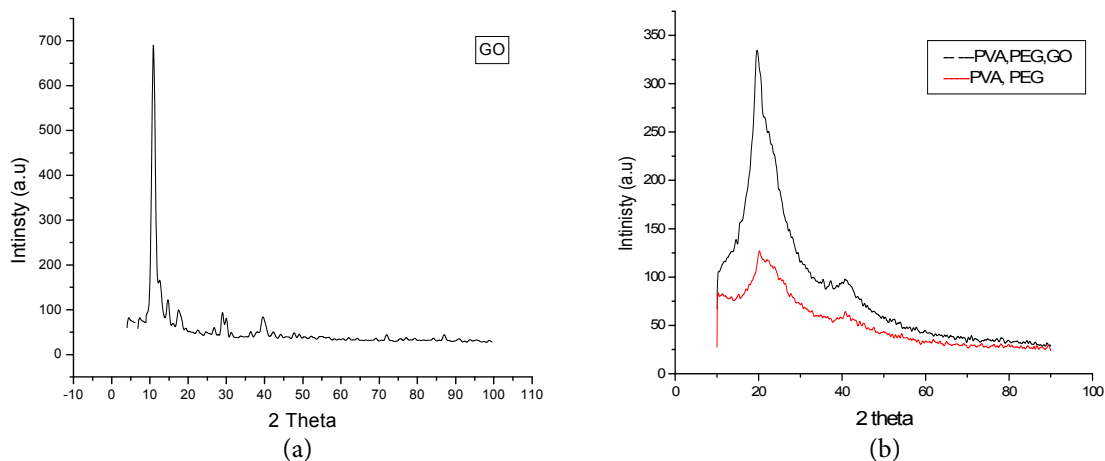


Fig. 4: XRD of GO (a) and (b) GO-PEG-PVA, PVA-PEG hydrogel.

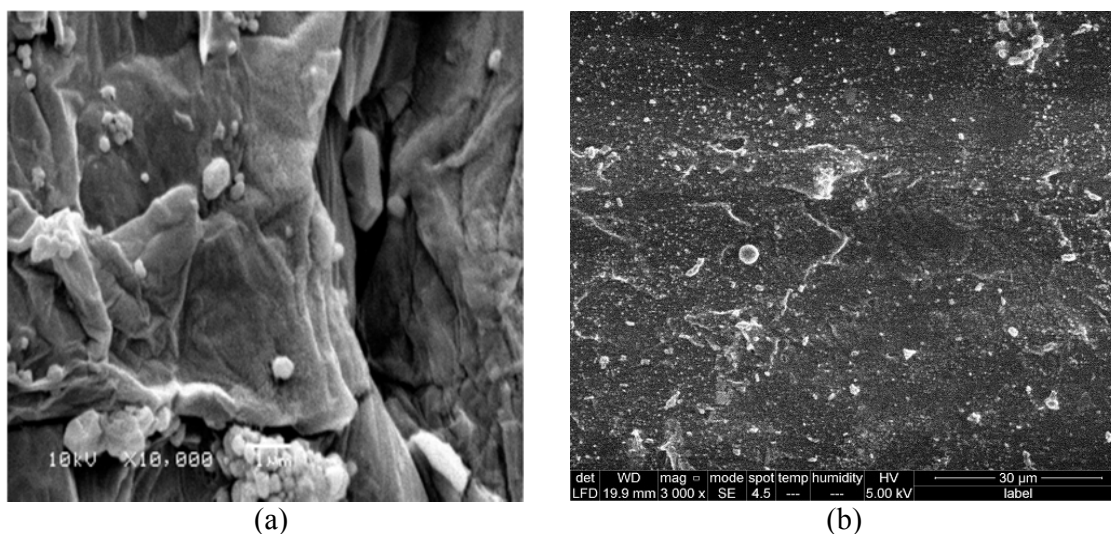


Fig. 5: (a) SEM micrograph of graphene oxide, (b) GO-PEG-PVA composite hydrogel.

wrinkled and kinked areas. On the other hand, the SEM image of PVA-PEG-GO composite hydrogel (Fig. 5b) shows the uniform dispersion of GO in the polymer matrices.

Batch Experiment

Effect of pH

It is well known that adsorption of Cu^{2+} ions from its water solution onto adsorbents depends on the pH value of the solution. The adsorption characteristics of Cu^{2+} ions on graphene oxide with various pH values ranging 1.0–7.0 were studied using an initial Cu^{2+} ions concentration of 500 mg l^{-1} . The results are reported in Fig. 6, which shows that the uptake of Cu^{2+} ions increased when the pH increased from 3.0 to 5.0.

The removal efficiency of GO, hydrogel with GO and hydrogel without GO increases with the increase of the pH value from 1 to reach a maximum of pH 5 and a decrease when the pH increases to 7. The results in case of GO can be explained based on the competition between Cu^{2+} ions and H_3O^+ for adsorption sites on GO. At low pH levels, an excess H_3O^+ competes with Cu^{2+} ions resulting in a low level of adsorbed Cu^{2+} ions. When the pH value increased, the covered H_3O^+ ions left the GO surface and made the sites available to Cu^{2+} ions. This condition suggests that an ion-exchange mechanism ($\text{H}^+/\text{Cu}^{2+}$) may be included in the adsorption of Cu^{2+} ions [46,47]. In addition, the negative charge on the surface of GO increased because the oxygen-containing functional groups became deprotonated with the increase in pH value. Hence, the electrostatic attraction between

GO and Cu^{2+} ions was enhanced, hence further increasing the adsorption amount of Cu^{2+} ions.

While in the case of hydrogels, the adsorption of heavy metals was inhibited at low pH values. When the pH value was above 3.0, the adsorption efficiencies reached the adsorption balance points of Cu^{2+} ions, the optimum value was reached at pH 5. It is reasonable to say that at low pH values, there weren't any charges on the surface of the hydrogel. Therefore, the positive metal ions are difficult to adsorb on the surface of hydrogel-GO or the surface may be coated with H_3O^+ ions, so the positive metal ions are difficult to adsorb on the positively charged surface of the electrostatic repulsion [26]. However, the charged surface of the hydrogel (negative charge) increased with the increase of the pH value. So the combination of metal ions and hydroxyl groups on the PVA, PEG-GO gel became dominant and thereby resulted in the increase of metal ion sorption.

Effect of contact time

The relationship between the adsorption behavior of Cu^{2+} ions on adsorbents GO, PVA-PEG-GO and PVA-PEG hydrogels and the contact time were investigated using an initial Cu^{2+} ions concentration of 500 mg l^{-1} at optimum pH 5.0, the result is represented in Fig. 7. It was found that the adsorption capacity of GO and both hydrogels increased with increasing the time due to the existence of many binding sites for Cu^{2+} ions. The adsorption capacity gradually increased and finally remained constant, and the adsorption equilibrium occurred after stirring

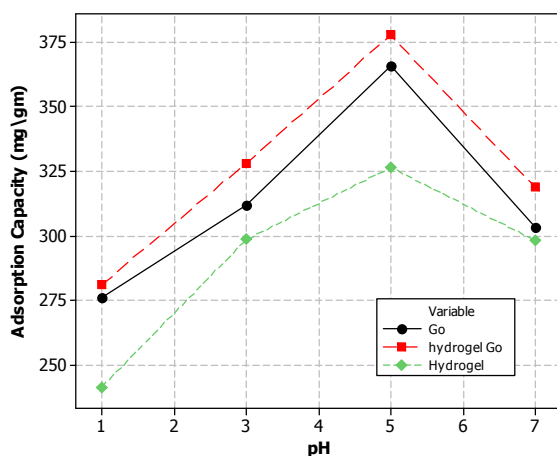


Fig. 6: Effect of initial solution pH on adsorption uptake of Cu(II) (initial Cu(II) concentration 500 mg l^{-1} , dosage of GO 100 mg l^{-1} , contact time 60 min)

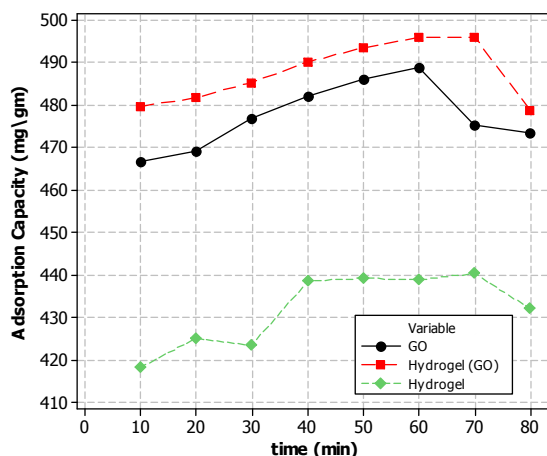


Fig. 7: Effect of contact time on adsorption of Cu(II) (initial Cu(II) mass concentration 500 mg l^{-1} , dosage of GO 100 mg l^{-1} , initial solution pH 5.0)

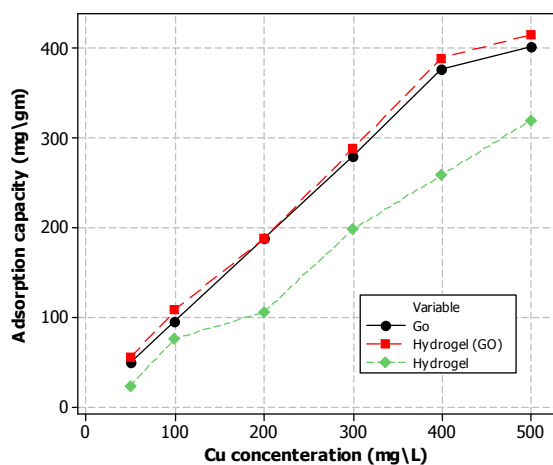


Fig. 8: Effect of Cu Concentration (initial dosage of GO 0.2 mg mL⁻¹, initial solution pH 5.0).

for 60 minutes. The delay in time of desorption may attribute to the weakening of the driving force resulting in the decrease of available adsorption sites and pH values. These decreased as a consequence of releasing H⁺ from the oxygen-containing functional groups (COOH or OH) on the surface of GO and hydrogels to the solution, hence hindering adsorption. Therefore, the adsorption time was fixed at 60 minutes in subsequent adsorption experiments to make sure that the equilibrium is reached [48].

Effect of initial concentration on Cu²⁺ ions adsorption

The uptake of Cu²⁺ ions highly depended on the initial concentration of Cu²⁺ ions (Fig. 8). It is

obvious that the adsorption capacity increased with the increase of initial Cu²⁺ ions' concentration. The adsorption capacity of GO-PVA-PEG hydrogel is higher than GO only and PVA-PEG hydrogel. The adsorption capacity of GO-PVA-PEG hydrogel increased from 55.4 to 415 mg g⁻¹ when the initial Cu²⁺ ions' concentration increased from 50 to 500 mg g⁻¹, while the adsorption capacity for GO and the PVA-PEG hydrogel increased from 50 to 400 mg g⁻¹ and 23.46 to 325 mg g⁻¹, respectively.

Adsorption kinetic studies

Studies the kinetic data were analyzed using two commonly kinetic models, the pseudo-first-order [44] and the pseudo-second-order [45], which can be expressed in the linear forms as follows:

$$\log(q_e - q_t) = \log(q_e) - \frac{k_1}{2.303}(t) \quad (3)$$

$$\frac{t}{q_t} = \frac{1}{k_2 q_e^2} + \frac{1}{q_e}(t) \quad (4)$$

where q_e and q_t are the adsorption capacity at equilibrium and time t , respectively (mg g⁻¹), k_1 (min⁻¹) is rate constant of pseudo-first order adsorption, while k_2 (g/mg min) is rate constant of pseudo-second order adsorption. The adsorption kinetic plots are shown in Fig. 9(a,b) and the related parameters calculated from the two models are listed in Table 1. The values of the correlation coefficients indicate that the adsorption kinetics fits better to the pseudo-second-order model rather than to the pseudo-first-order model.

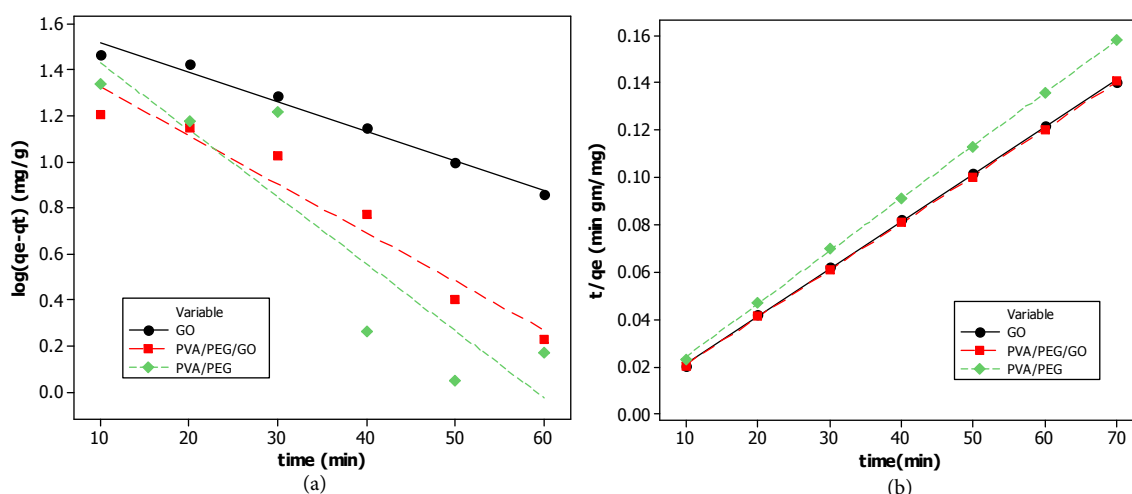


Fig. 9: (a) Pseudo first order model, (b) pseudo second order model for GO, PVA/PEG/GO, PVA/PEG at initial concentration of Cu²⁺ = 500 mg l⁻¹, dosage of GO 100 mg l⁻¹, initial solution pH 5.0).

Adsorption isotherms

An adsorption isotherm expresses the relationship between the amount of adsorbate adsorbed per unit weight of adsorbent (Q_e , mg g^{-1}) and the concentrations of adsorbate in the bulk solution (C_e , mg l^{-1}) at a given temperature under equilibrium conditions. As well as it shows the quality of an adsorbent by how much adsorbate it can sorb and keep in an immobilized form [46]. The experimental data were analyzed using the Langmuir and Freundlich adsorption isotherm models. The Langmuir isotherm model describes an ideal adsorption process, which contains the formation of a uniform single layer adsorbate on the outer surface of the adsorbent [20]. The Langmuir model was based on monolayer adsorption and could be described as the following equation:

$$\frac{C_e}{q_e} = \frac{1}{k_L Q_m} + \frac{1}{Q_m} C_e \quad (5)$$

where C_e (mg l^{-1}) is the equilibrium concentration of adsorbate, q_e (mg g^{-1}) is the amount of metal adsorbed per gram of the adsorbent at equilibrium, Q_m (mg g^{-1}) is the maximum monolayer coverage capacity and k_L (l mg^{-1}) is the Langmuir isotherm constant determined by plotting C_e/q_e versus C_e .

The Freundlich isotherm model describes the adsorption on a heterogeneous surface with un-uniform energy. The Freundlich isotherm can be described as the following linear equation:

$$\log q_e = \log k_F + \frac{1}{n} \log C_e \quad (6)$$

where k_F (mg g^{-1}) is the Freundlich isotherm constant and n is the adsorption intensity. Fig. 10 (a,b) show Langmuir and Freundlich adsorption isotherm models. The parameter values of Langmuir and Freundlich model could be determined by the linear relationship of $C_e/q_e - C_e$ and $\log q_e - \log C_e$, respectively and the results are presented in Table 2. The Higher correlation coefficient of Langmuir isotherm model for GO implied that monolayer adsorption was more readily to occur on the homogeneous surface of graphene oxide sheets. While Freundlich model was more fit to PVA-PEG-GO and PVA-PEG hydrogel. The maximum adsorption capacity (Q_m) was in order PVA-PEG-GO (917 mg g^{-1}) > GO (900 mg g^{-1}) > PVA-PEG (412 mg g^{-1}) (Table 2) and they are compared with another adsorbent in Table 3. The adsorption obeys Freundlich isotherm models for PVA-PEG-GO and n value > 1 so the adsorption is physical adsorption.

Table 1: Parameters of kinetic models

Adsorbent	q_e exp mg g^{-1}	Pseudo-first order			Pseudo-second order		
		K_1 (l min^{-1})	q_e Cal.	R^2	K_2	q_e Cal. mg g^{-1}	R^2
GO	496.46	0.027	44.4	0.98	2.79×10^{-3}	500	0.999
PVA-PEG-GO	495.16	0.048	34.5	0.94	4×10^{-3}	502	0.999
PVA-PEG	440	0.066	52.9	0.823	2.78×10^{-3}	444.5	0.999

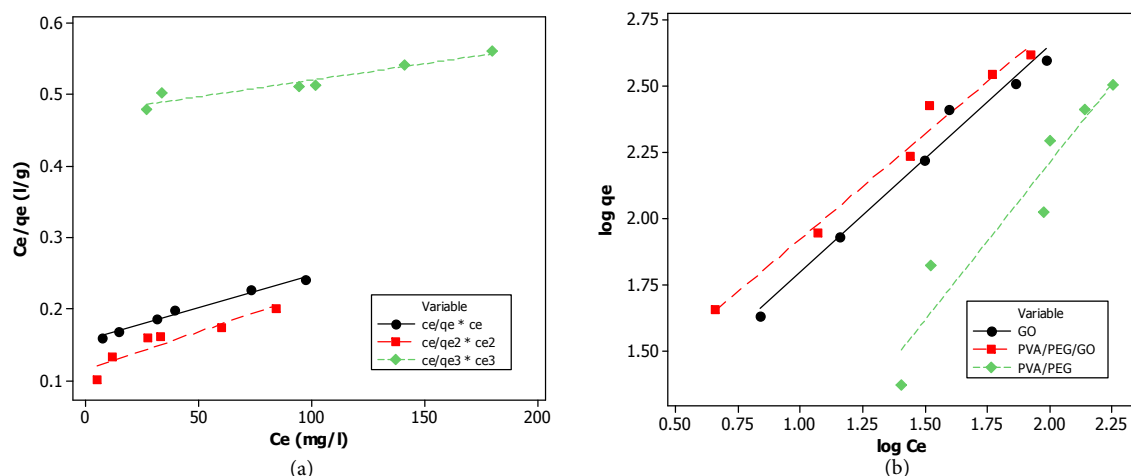


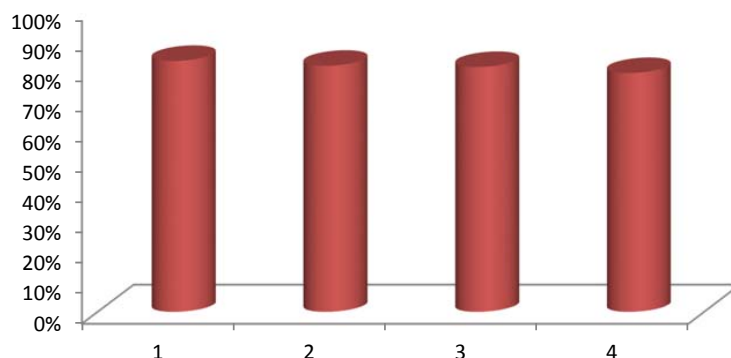
Fig. 10: (a) Langmuir and (b) Freundlich adsorption isotherm models of Cu (II) on GO, PVA-PEG-GO, and PVA-PEG.

Table 2: Fitting parameters for Langmuir and Freundlich isotherms

Model	GO	PVA-PEG-GO	PVA-PEG
Linear Langmuir			
Q_m (mg/g)	900	917	423
k_a (l/mg)	5.76×10^{-3}	10.23×10^{-3}	0.9×10^{-3}
R_l	0.257	0.163	0.68
R^2	0.992	0.92	0.959
Linear Freundlich			
n	1.169	1.26	0.839
k_F	8.74	13.45	0.671
R^2	0.969	0.990	0.993

Table 3: Comparison of maximum adsorption capacity of Cu (II) on various adsorptions

Adsorbent	Maximum Capacity (mg g ⁻¹)	Reaction condition	Ref
Sulfonated magnetic GO	62.73	At initial Cu(II) conc. 60 mg/l, pH=6, time 30 min, and Temp=25±1	46
Graphene oxide	117.5	At initial Cu(II) conc. 20 mg/l, pH=5, time 150 min, and Temp=25±1	47
EDTA-MGO	301.2	At initial Cu(II) conc. 100 mg/l, pH=5.1, time 90 min, and Temp=25±1	48
graphene oxide-ethylenediamine triacetic acid	108.7	At initial Cu(II) conc. 20 mg/l, pH=5, time 90 min, and Temp=25±1	49
GO	909.0	At initial Cu(II) conc. 500 mg/l, pH=5, time 60 min, and Temp=25±1	This work
PVA-PEG-GO hydrogel	917	At initial Cu(II) conc. 500 mg/l, pH=5, time 60 min, and Temp=25±1	This work

Fig. 11: Effect of recycle times on the Cu²⁺ ions removal efficiency of GO-PEG-PVA hydrogel.

Recyclability test

The industrial applicability of adsorbents depends not only on the adsorption capacity but also on the desorption regeneration. Treatment of the GO-PVA-PEG hydrogel by diluted HCl lead to large amounts of H⁺ which caused protonation of hydroxyl groups of polyvinyl alcohol and polyethylene glycol. Therefore, metal ions can be replaced by H⁺. After experiencing each adsorption

cycle, the metal-adsorbed by GO-PVA-PEG hydrogel was eluted with 0.1 M HCl solution, then neutralized by 0.1 M NaOH solution and finally washed with double distilled water for the next cycle [26]. Fig. 11 exhibits the reusability of GO-PVA-PEG hydrogel in removing Cu²⁺ ions. The removal efficiencies are 83% for the first cycle and about 81.4, 81, and 79 % for the second, third and fourth cycle, respectively. That proves the

efficient reusability of the newly prepared hydrogel. Recycling with HCl decreased the pH value which leads to enhancing polymers cross-linking and decreased the hydrogel degradation.

CONCLUSIONS

The graphene oxide was prepared by oxidizing purified natural flake graphite via the modified Hummer's method; the PVA-PEG-GO nanocomposites were prepared by a simple and environmentally friendly process that used water as the proceeding medium. The results of FTIR showed that graphite is oxidized by strong oxidants and that oxygen atoms are introduced into the graphite layers to form C=O, C-H, COOH and C-O-C bonds. FTIR of the hydrogel showed the interaction of GO with both polymers, PVA and PEG. The XRD results of GO show 2θ of 11.02° with interlayer spacing equal to 0.71 nm which attributed to good functionalization with hydroxyl groups. On the other hand, XRD of the hydrogel with GO showed the disappearance of the characteristic peak of GO and this emphasized the good dispersion of GO into the hydrogel. In addition to that, the characteristic peak of PVA decreased in the case of GO-PVA-PEG hydrogel due to a reduction in crystallinity. SEM image of GO-PVA-PEG hydrogel indicated the good dispersion of GO into the polymers. The adsorption obeys Freundlich isotherm models for PVA-PEG-GO, and the values of the correlation coefficients indicate that the adsorption kinetics fits better to the pseudo-second-order model rather than to the pseudo-first-order model. The present study clearly shows that GO-PVA-PEG hydrogel is effective in the removal of Cu^{2+} ions from water without leaving any toxic residual. It also proved how GO-PVA-PEG hydrogel is of good reusability, revealing its potential in practical application.

CONFLICT OF INTEREST

The authors declare that there is no conflict of interests regarding the publication of this manuscript.

REFERENCES

1. El-Nemr A. Impact, Monitoring, and Management of Environmental Pollution (Pollution Science, Technology & Abatement Series): Nova Science Publishers Incorporated; 2010.
2. Fayyaz F, Rahimi R, Rassa M, Maleki A. Efficient photo-oxidation of phenol and photo-inactivation of bacteria by cationic tetrakis(trimethylanilinium)porphyrins. *Water Science and Technology: Water Supply*. 2015;15(5):1099-1105.
3. Khaled A, El Nemr A, El Sikaily A. Heavy Metals Concentrations in Biota of the Mediterranean Sea: A Review, Part I. *Blue Biotechnology Journal*. 2013;2(1):79.
4. Khaled A, El Nemr A, El Sikaily A. HEAVY METAL CONCENTRATIONS IN BIOTA OF THE MEDITERRANEAN SEA: A REVIEW, PART II. *Blue Biotechnology Journal*. 2013;2(2):191.
5. Maleki A, Rahimi R, Maleki S. Efficient oxidation and epoxidation using a chromium(VI)-based magnetic nanocomposite. *Environ Chem Lett*. 2016;14(2):195-9.
6. El-Nemr A. Non-conventional Textile Waste Water Treatment: Nova Science Publishers; 2012.
7. Abdelwahab O, El Sikaily A, Khaled A, El Nemr A. Mass-transfer processes of chromium(VI) adsorption onto guava seeds. *Chem Ecol*. 2007;23(1):73-85.
8. El Nemr A, El Sikaily A, Khaled A, Abdelwahab O. Removal of toxic chromium(VI) from aqueous solution by activated carbon using *Casuarina equisetifolia*. *Chem Ecol*. 2007;23(2):119-29.
9. El-Sikaily A, Nemr AE, Khaled A, Abdelwehab O. Removal of toxic chromium from wastewater using green alga *Ulva lactuca* and its activated carbon. *J Hazard Mater*. 2007;148(1):216-28.
10. El Nemr A. Pomegranate husk as an adsorbent in the removal of toxic chromium from wastewater. *Chem Ecol*. 2007;23(5):409-25.
11. Nemr AE. Potential of pomegranate husk carbon for Cr(VI) removal from wastewater: Kinetic and isotherm studies. *J Hazard Mater*. 2009;161(1):132-41.
12. Sun L, Fugetsu B. Mass production of graphene oxide from expanded graphite. *Mater Lett*. 2013;109:207-10.
13. Sun L, Fugetsu B. Effect of encapsulated graphene oxide on alginate-based bead adsorption to remove acridine orange from aqueous solutions. *arXiv preprint arXiv:13070223*. 2013.
14. Zhao G, Li J, Ren X, Chen C, Wang X. Few-Layered Graphene Oxide Nanosheets As Superior Sorbents for Heavy Metal Ion Pollution Management. *Environ Sci Technol*. 2011;45(24):10454-62.
15. Maleki A, Rahimi R, Maleki S. Efficient oxidation and epoxidation using a chromium(VI)-based magnetic nanocomposite. *Environ Chem Lett*. 2016;14(2):195-9.
16. Maleki A, Paydar R. Bionanostructure-catalyzed one-pot three-component synthesis of 3,4-dihydropyrimidin-2(1H)-one derivatives under solvent-free conditions. *React Funct Polym*. 2016;109(Supplement C):120-4.
17. Najafian A, Rabbani M, Rahimi R, Deilamkamar M, Maleki A. Synthesis and characterization of copper porphyrin into SBA-16 through "ship in a bottle" method: A catalyst for photo oxidation reaction under visible light. *Solid State Sci*. 2015;46(Supplement C):7-13.
18. Mahboubbeh Rabbani, Hamideh Bathaee, Rahmatollah Rahimi, Maleki A. Photocatalytic degradation of p-nitrophenol and methylene blue using Zn-TCPP/Ag doped mesoporous TiO_2 under UV and visible light irradiation. *Desalin Water Treat*. 2016;57(53):25848-56.
19. Zhao G, Ren X, Gao X, Tan X, Li J, Chen C, et al. Removal of Pb(II) ions from aqueous solutions on few-layered graphene oxide nanosheets. *Dalton Trans*. 2011;40(41):10945-52.
20. Travlou NA, Kyzas GZ, Lazaridis NK, Deliyanni EA. Graphite oxide/chitosan composite for reactive dye removal. *CHEM ENG J*. 2013;217(Supplement C):256-65.

21. Zhu J, Wang Y, Liu J, Zhang Y. Facile One-Pot Synthesis of Novel Spherical Zeolite-Reduced Graphene Oxide Composites for Cationic Dye Adsorption. *IND ENG CHEM RES.* 2014;53(35):13711-7.
22. González JA, Villanueva ME, Piehl LL, Copello GJ. Development of a chitin/graphene oxide hybrid composite for the removal of pollutant dyes: Adsorption and desorption study. *CHEM ENG J.* 2015;280(Supplement C):41-8.
23. Ma Z, Liu D, Zhu Y, Li Z, Li Z, Tian H, et al. Graphene oxide/chitin nanofibril composite foams as column adsorbents for aqueous pollutants. *Carbohydr Polym.* 2016;144(Supplement C):230-7.
24. Jamnongkan T, Kantarot K, Niemtang K, Pansila PP, Wattanakornsiri A. Kinetics and mechanism of adsorptive removal of copper from aqueous solution with poly(vinyl alcohol) hydrogel. *T NONFERR METAL SOC.* 2014;24(10):3386-93.
25. Fan L, Luo C, Li X, Lu F, Qiu H, Sun M. Fabrication of novel magnetic chitosan grafted with graphene oxide to enhance adsorption properties for methyl blue. *J Hazard Mater.* 2012;215(Supplement C):272-9.
26. Kong X-b, Tang Q-y, Chen X-y, Tu Y, Sun S-z, Sun Z-l. Polyethylene glycol as a promising synthetic material for repair of spinal cord injury. *Neural Regener Res.* 2017;12(6):1003-8.
27. Xu R, Zhou G, Tang Y, Chu L, Liu C, Zeng Z, et al. New double network hydrogel adsorbent: Highly efficient removal of Cd(II) and Mn(II) ions in aqueous solution. *CHEM ENG J.* 2015;275(Supplement C):179-88.
28. Abraham TN, Kumar R, Misra RK, Jain SK. Poly(vinyl alcohol)-based MWCNT hydrogel for lead ion removal from contaminated water. *J Appl Polym Sci.* 2012;125(S1):E670-E4.
29. Khokan Chandra Sarker, Ullaha R. Determination of Trace Amount of Cu(II) Using UV-Vis. Spectrophotometric Method. *International Journal of Chemical Studies.* 2013;1(1):5-14.
30. Niyogi S, Bekyarova E, Itkis ME, McWilliams JL, Hamon MA, Haddon RC. Solution Properties of Graphite and Graphene. *J Am Chem Soc.* 2006;128(24):7720-1.
31. Hirata M, Gotou T, Horiuchi S, Fujiwara M, Ohba M. Thin-film particles of graphite oxide 1:: High-yield synthesis and flexibility of the particles. *CARBON.* 2004;42(14):2929-37.
32. Lerf A, He H, Forster M, Klinowski J. Structure of Graphite Oxide Revisited. *The Journal of Physical Chemistry B.* 1998;102(23):4477-82.
33. He H, Klinowski J, Forster M, Lerf A. A new structural model for graphite oxide. *Chem Phys Lett.* 1998;287(1):53-6.
34. Cote LJ, Kim F, Huang J. Langmuir-Blodgett Assembly of Graphite Oxide Single Layers. *J Am Chem Soc.* 2009;131(3):1043-9.
35. Cai D, Song M. Preparation of fully exfoliated graphite oxide nanoplatelets in organic solvents. *J Mater Chem.* 2007;17(35):3678-80.
36. Paredes JI, Villar-Rodil S, Martínez-Alonso A, Tascón JMD. Graphene Oxide Dispersions in Organic Solvents. *LANGMUIR.* 2008;24(19):10560-4.
37. Song J, Wang X, Chang C-T. Preparation and Characterization of Graphene Oxide. *Journal of Nanomaterials.* 2014;2014:6.
38. Thakur S, Karak N. Green reduction of graphene oxide by aqueous phytoextracts. *CARBON.* 2012;50(14):5331-9.
39. Du Q, Zheng M, Zhang L, Wang Y, Chen J, Xue L, et al. Preparation of functionalized graphene sheets by a low-temperature thermal exfoliation approach and their electrochemical supercapacitive behaviors. *Electrochim Acta.* 2010;55(12):3897-903.
40. Ali ZI, Eisa WH. Characterization of Electron Beam Irradiated Poly Vinyl Alcohol/Poly Ethylene Glycol Blends. *Journal of Scientific Research.* 2013;6(1):29-42.
41. Gadea JL, Cesteros LC, Katime I. Chemical-physical behavior of hydrogels of poly(vinyl alcohol) and poly(ethylene glycol). *Eur Polym J.* 2013;49(11):3582-9.
42. Mansur HS, Oréfice RL, Mansur AAP. Characterization of poly(vinyl alcohol)/poly(ethylene glycol) hydrogels and PVA-derived hybrids by small-angle X-ray scattering and FTIR spectroscopy. *POLYMER.* 2004;45(21):7193-202.
43. Fu C, Zhao G, Zhang H, Li S. Evaluation and characterization of reduced graphene oxide nanosheets as anode materials for lithium-ion batteries. *Int J Electrochem Sci.* 2013;8:6269-80.
44. Tang C-M, Tian Y-H, Hsu S-H. Poly(vinyl alcohol) Nanocomposites Reinforced with Bamboo Charcoal Nanoparticles: Mineralization Behavior and Characterization. *Materials.* 2015;8(8):4895-911.
45. Rengaraj S, Joo CK, Kim Y, Yi J. Kinetics of removal of chromium from water and electronic process wastewater by ion exchange resins: 1200H, 1500H and IRN97H. *J Hazard Mater.* 2003;102(2):257-75.
46. Mi X, Huang G, Xie W, Wang W, Liu Y, Gao J. Preparation of graphene oxide aerogel and its adsorption for Cu²⁺ ions. *CARBON.* 2012;50(13):4856-64.
47. Yang Y, Wu W-q, Zhou H-h, Huang Z-y, Ye T-t, Liu R, et al. Adsorption behavior of cross-linked chitosan modified by graphene oxide for Cu(II) removal. *Journal of Central South University.* 2014;21(7):2826-31.
48. Cui L, Wang Y, Gao L, Hu L, Yan L, Wei Q, et al. EDTA functionalized magnetic graphene oxide for removal of Pb(II), Hg(II) and Cu(II) in water treatment: Adsorption mechanism and separation property. *CHEM ENG J.* 2015;281(Supplement C):1-10.
49. Mejias Carpio IE, Mangadlao JD, Nguyen HN, Advincula RC, Rodrigues DE. Graphene oxide functionalized with ethylenediamine triacetic acid for heavy metal adsorption and anti-microbial applications. *CARBON.* 2014;77(Supplement C):289-301.